INTERNATIONAL JOURNAL OF
COASTAL, OFFSHORE & ENVIRONMENTAL ENGINEERING IJCOE Vol.10/No. 4/ Autumn 2025 (45-54)

Available online at: www. Ijcoe.org

Field Investigation of Water Mass Stratification and Variability in the Strait of Hormuz

Samad Hamzei*[1], Amirmahdi Zarboo[1], Emad Koochaknejad[1]

[1] *Iranian National Institute for Oceanography and Atmospheric Sciences (INIOAS), Tehran, 1411813389, Iran*
sh_hamzei@yahoo.com , amirmahdizarboo@gmail.com, emad.koochaknejad@inio.ac.ir

ARTICLE INFO

Article History:
Received: 16 Sep 2025
Accepted: 5 Nov 2025

Keywords:
Persian Gulf water mass
Indian Ocean water mass
Seasonal thermocline
Water stratification
Strait of Hormuz

ABSTRACT

The Persian Gulf is a shallow basin characterized by high evaporation rates, resulting in the formation of one of the saltiest water bodies in the world. To compensate for the evaporative water loss, a less saline water mass enters the Gulf through the Strait of Hormuz, known as the Indian Ocean Surface Water (IOSW). Due to its high density, the hypersaline Persian Gulf Water (PGW) sinks toward the seabed and exits the Gulf through the deeper layers of the Strait of Hormuz, flowing toward the Gulf of Oman. To identify and characterize the water masses present in the Persian Gulf, Strait of Hormuz, and Gulf of Oman, hydrographic surveys were conducted during the summer and winter seasons of the 2102 and 2201 expeditions aboard the Persian Gulf Explorer. Using CTD profiling, physical and chemical parameters of seawater were measured. Analysis of temperature, salinity, and potential density anomaly across isopycnal layers—surface, intermediate, and deep—along north-south and east-west vertical transects enabled the evaluation of water mass structure and distribution in the region. Results indicate that during summer, surface water mixing is intense due to atmospheric conditions such as the monsoon, and stratification primarily occurs below depths of 30 meters. In contrast, winter stratification weakens, and due to lower temperatures, horizontal layering is observed from the eastern Strait of Hormuz to the western end of the Persian Gulf—marked by increasing salinity and density, and decreasing temperature. The IOSW enters the Persian Gulf through the Strait of Hormuz and propagates along the northern coastline. In summer, cyclonic eddies in the Gulf induce southward flow in several central regions. The PGW is observed in the deep central Gulf during summer, while surface mixing between IOSW and Gulf waters reduces salinity in the upper layers. The summer PGW mass is detectable in the western Gulf of Oman at approximately 100 meters depth near the Strait of Hormuz. However, in winter, the inflow into the Gulf weakens due to reduced wind forcing and strong horizontal stratification of salinity and density, which limits the penetration of incoming water.

1. Introduction

The Persian Gulf is considered the third largest gulf in the world, following the Gulf of Mexico and Hudson Bay. The Strait of Hormuz is one of the most strategic maritime corridors globally, serving as the primary gateway for oil exports and a major route for non-oil trade between Southeast Asia and the Middle East. Together, the Persian Gulf and the Gulf of Oman form a vital geopolitical and commercial zone for Iran, encompassing diverse marine ecosystems and substantial oil and gas reserves (Raeisi et al., 2020).

The Persian Gulf is a shallow, semi-enclosed basin with an average depth of 35 meters and a maximum depth of 90 meters, connected to the Gulf of Oman via the Strait of Hormuz. It is recognized as one of the principal sources of hypersaline water masses in the global ocean. The Gulf of Oman, located in the northwestern part of the Indian Ocean near the Arabian Sea, has an L-shaped configuration. The Strait of

Hormuz lies approximately at 26°30′N and 56°30′E, with a width of 56 km and depths ranging from 90 to 110 meters. The regional meteorology is dominated by northwesterly winds with seasonal variability, which also influence the Gulf of Oman. Sea surface temperatures in the Strait of Hormuz range from 32–34°C in summer and 18–20°C in winter. Due to high evaporation rates exceeding freshwater input from precipitation and river discharge, the Persian Gulf functions as a reverse estuary (Reynolds, 1993).

Geographically, the Persian Gulf extends in a northwest–southeast direction between 25°–30°N and 48°–56°E, while the Gulf of Oman spans 26°–32°N and 56°–62°E. Although the maximum depth of the Persian Gulf is 90 meters, depths exceeding 100 meters are observed in the Strait of Hormuz. Pous et al. (2004) conducted hydrographic measurements in the eastern Strait of Hormuz during October and early November 1999, analyzing physical water properties, current profiles, sea level fluctuations, and surface circulation. Their findings indicated that inflow to the Persian Gulf occurs through the northern sector of the strait, while dense Persian Gulf Water (PGW) exits through the southern deep layers.

In more recent studies, Azizpour et al. (2016) deployed four subsurface mooring systems during field campaigns in November 2012 and January 2013, identifying tidal dynamics in the Strait of Hormuz as a combination of semi-diurnal and diurnal standing wave patterns. Hunter (1982), using data from a UK meteorological vessel in 1981, observed a surface inflow of approximately 0.1 m/s along the Iranian coast. Seasonal analysis revealed stronger inflow during summer (~0.2 m/s) and weaker currents in autumn and winter. These estimates were supported by ship drift observations along the Iranian coastline.

Sonu (1979), based on April 1977 measurements, documented an inflow penetrating up to 200 km into the Persian Gulf via the Strait of Hormuz. The density contrast between the Persian Gulf and the Gulf of Oman, intensified by the summer monsoon, drives water exchange, as previously noted by Schott (1918), Barlow (1932), and others. The outflow of PGW into the Gulf of Oman has been reported by Sewell (1934), Emery (1956), Duing & Koske (1967), and more recently by Ramak (2022).

Sugden (1963) proposed a surface inflow above the outflow layer, accompanied by cyclonic circulation within the Persian Gulf. Pous et al. (2004) confirmed that PGW exits through the southern deep layers of the strait, while IOSW enters through the northern sector. Their 1999 GOGP99 cruise data revealed that PGW outflow follows a southeastward trajectory below 200 meters in the Gulf of Oman, later deflecting southwestward near the continental slope and continuing along the Omani coast at ~0.2 m/s. Temperature and salinity of PGW decrease from 27°C and 39.75 psu in the Gulf to 21°C and 37.1 psu in the northern Arabian Sea, with non-uniform mixing in localized regions.

Five major water masses were identified:

- Seasonal Thermocline Water (TW): ~30°C, 37 psu at ~25 m depth (summer)
- Indian Ocean Surface Water (IOSW): 20–22°C, 36–36.5 psu at 50–100 m
- Persian Gulf Water (PGW): 20–22°C, 37.25–37.5 psu at 150–300 m
- Red Sea Water (RSW): 10–12°C, 35.5 psu at ~800 m
- North Indian Deep Water (NIDW): ~2°C, 34.8 psu at 2000–4000 m

Hunter (1982) attributed PGW formation to intense evaporation in the northwest Gulf, with PGW descending and moving southward under the influence of Coriolis deflection. He noted that sea level reduction due to evaporation and limited rainfall is compensated by inflow along the Iranian coast from the Gulf of Oman.

2. Methodology

To investigate the spatial distribution and interaction of water masses in the Strait of Hormuz, data from two hydrographic cruises conducted in 2021 (1400 SH) were analyzed.

The summer cruise, titled “Oceanographic Monitoring of the Persian Gulf and Gulf of Oman,” was conducted by the Iranian National Institute for Oceanography and Atmospheric Science aboard the Persian Gulf Explorer during September–October 2021 (PGE2102). Measurements were taken at 67 stations from the Arvand River mouth (Sept 7) to Chabahar (Oct 1).

The winter cruise, also titled “Oceanographic Monitoring of the Persian Gulf and Gulf of Oman,” was conducted in two legs during January–February 2022 (PGE2201). A total of 86 stations were sampled from the northernmost point of the Persian Gulf (Jan 12) to near Chabahar (Feb 12), under varying atmospheric and oceanic conditions.

Table 1. Specifications of CTD Measurements Conducted During Research Cruises

Cruise Code	Survey Area	Number of Stations	Measurement Period
PGE2102	Persian Gulf, Strait of Hormuz, Gulf of Oman	67	September 7 to October 1, 2021
PGE2201	Persian Gulf, Strait of Hormuz, Gulf of Oman	86	January 12 to February 12, 2022

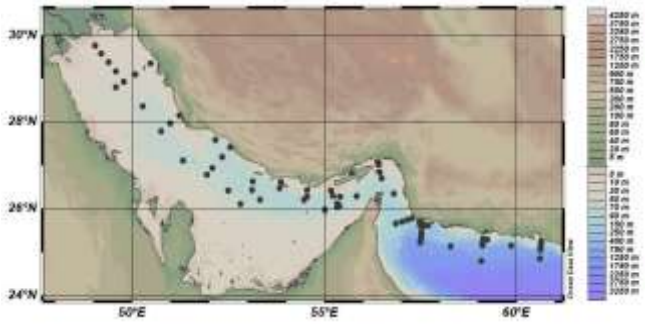

Figure 1. Locations of Sampling Stations During summer and winter Cruises

Through the analysis of temperature, salinity, and density fields, the distinct characteristics and boundaries of various water masses were identified. By plotting isotherms, isohalines, and isopycnals across different depth layers, the spatial extent and presence of water masses were delineated using contour mapping. For this purpose, a depth of 5 meters was selected to represent the surface layer, and 50 meters for the deep layer of the Persian Gulf.

Using vertical profiles of temperature, salinity, and density, the location, intrusion extent, and lens-like structure of water masses were determined. These profiles were extracted along east–west transects across the central Strait of Hormuz and north–south transects across the western, central, and eastern sectors of the strait.

3. Results and Discussion

Water masses are generally classified into deep and bottom waters, intermediate waters, and surface waters. Their nomenclature and spatial boundaries vary depending on the oceanic basin in which they form. To identify and trace water masses, researchers rely on tracers, their position relative to the global ocean, and their vertical distribution (Emery and Meincke, 1986).

This section focuses on the identification and tracking of water masses, as well as the analysis of horizontal and vertical mixing and stratification in the Persian Gulf and Gulf of Oman during warm and cold seasons, based on CTD measurement data.

3.1. Salinity Fields

Figure 2 illustrates isohaline distributions at depths of 5 meters and 50 meters from the PGE2102 (summer) and PGE2201 (winter) research cruises. In summer, the highest salinity values are observed along the southern Arabian coastline and the northwestern sector of the Persian Gulf. Lower salinity values appear in the central Gulf and along the northern coast of the Strait of Hormuz. In the Gulf of Oman, surface salinity is generally below 37 psu, while salinity in the Strait of Hormuz approaches 38 psu, and in the Persian Gulf ranges from 39 to 40 psu.

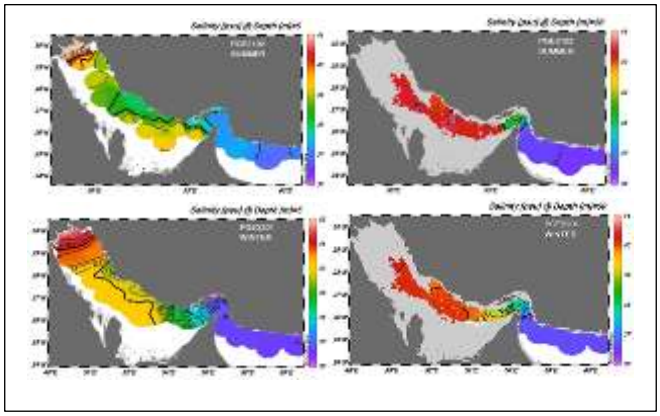

Figure 2. Isohaline surfaces in the Persian Gulf and the Gulf of Oman at depths of 5 and 50 meters during cruise PGE2102 in summer and cruise PGE2201 in winter

At 50 meters depth during summer, most areas of the Persian Gulf with depths exceeding 50 meters exhibit salinity values above 40 psu, with two distinct high-salinity cores located in the northern and central Gulf. A pronounced salinity gradient is evident in the western Strait of Hormuz, where salinity increases from 37.5 psu in the east to over 40 psu in the west. This depth reveals the interaction between the inflowing IOSW and the outflowing PGW, with a sharp salinity contrast clearly delineating the two water masses.

In winter, surface salinity data from PGE2201 show the highest values in the northwestern extremity of the Persian Gulf. Lower salinity is observed in the central and southern Gulf. In the Gulf of Oman, surface salinity drops below 36.8 psu, and in the northern Strait of Hormuz, it falls below 36 psu, attributed to heavy rainfall in January 2022, which introduced significant freshwater into the region.

At 50 meters depth, near-bottom waters in the Persian Gulf maintain salinity levels above 40 psu, but salinity decreases toward the Strait of Hormuz. In the Gulf of Oman, a more uniform salinity field is observed, with a clear east–west salinity gradient extending across the Strait of Hormuz.

3.2. Temperature Fields

Figure 3 presents isotherm distributions from cruises PGE2102 and PGE2201. Surface temperatures during the summer cruise (September–October 2021) exceed 35.5°C in the Persian Gulf, making it warmer than adjacent oceanic waters. In two northern zones near the Iranian coastline, temperatures reach up to 35°C. In the Strait of Hormuz, surface temperatures are more moderate, while in the Gulf of Oman, they drop below 31°C.

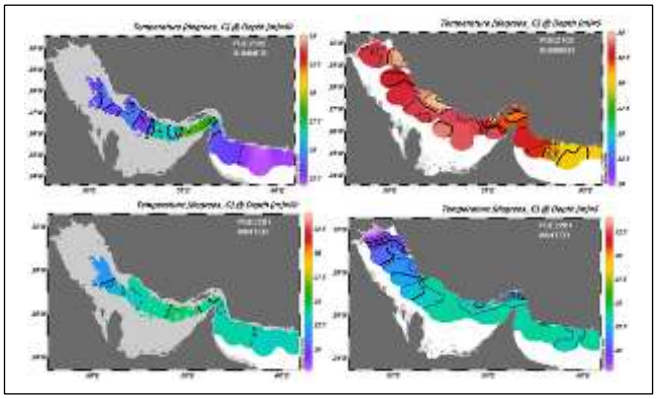

Figure 3. Isothermal surfaces in the Persian Gulf and the Gulf of Oman at depths of 5 and 50 meters during cruise PGE2102 in summer and cruise PGE2201 in winter

At 50 meters depth in summer, a noticeable temperature decline is observed in both the Persian Gulf and Gulf of Oman, whereas the Strait of Hormuz retains relatively higher temperatures. Temperatures fall below 25°C in the Persian Gulf and below 24°C in the Gulf of Oman, while the Strait of Hormuz shows values above 27°C. This pattern suggests enhanced vertical mixing in the Strait of Hormuz compared to the Persian Gulf and Gulf of Oman, resulting in a weaker summer thermocline in the strait.

Winter temperature variations across different depths reveal that at 5 meters, surface temperatures decrease from the central Gulf toward the northwestern end. From the central Gulf to the midsection of the Strait of Hormuz, temperatures remain relatively uniform, but in the northern coastal areas of the strait, temperatures drop to 20°C. The Gulf of Oman exhibits relatively homogeneous temperatures throughout. The strongest horizontal temperature gradients are found in the northwestern Persian Gulf and northern Strait of Hormuz.

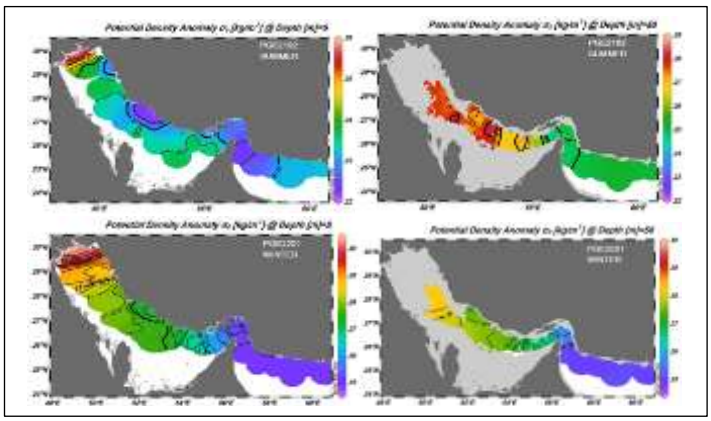

Figure 4. Isopycnal surfaces in the Persian Gulf and the Gulf of Oman at depths of 5 and 50 meters during cruise PGE2102 in summer and cruise PGE2201 in winter

At 50 meters depth in winter, temperatures vary slightly. Lower temperatures are observed in the central and northwestern Gulf, while warmer zones exceeding 24°C appear in the western and central Gulf, indicating the presence of a distinct water mass—likely the dense Persian Gulf Water (PGW)—characterized by its unique thermal signature.

3.3. Potential Density Anomaly (σ_0)

During the summer season, the highest values of potential density anomaly (σ_0) at the surface are observed in the northwestern Persian Gulf. Following this region, the southern sectors of the Gulf exhibit elevated density values, while the Strait of Hormuz and the central axis of the Gulf, near the Hormozgan–Bushehr boundary, show the lowest surface densities. Since seawater density is a function of both temperature and salinity, areas with higher salinity and lower temperature tend to exhibit greater potential density.

The lowest summer density values are recorded in the eastern Strait of Hormuz, but density increases again toward the Gulf of Oman and the Persian Gulf. This increase is attributed to higher salinity in the Gulf and lower surface temperatures in the Gulf of Oman compared to the Strait of Hormuz.

In winter, potential density anomaly at 5 meters depth shows maximum values in the northwestern Persian Gulf, reaching up to 30 kg/m³. From the Gulf toward the Strait of Hormuz, density decreases, stabilizing around 25.5 kg/m³ in the eastern Strait and adjacent Gulf of Oman. The strongest density gradients are observed in the western Strait of Hormuz and the northwestern Gulf.

At 50 meters depth, density anomaly in the Persian Gulf is generally higher than in the Strait of Hormuz and Gulf of Oman. However, due to the presence of warmer PGW in deeper layers, the density anomaly is not excessively high. In the Gulf of Oman, density values remain relatively uniform, but increase slightly toward the Strait of Hormuz.

3.4. Vertical Profiles

Figure 5 presents vertical sections T1, T2, and T3 across the western, central, and eastern Strait of Hormuz, and section L1 spanning west to east across the Persian Gulf, constructed to identify water masses and their interactions during summer and winter.

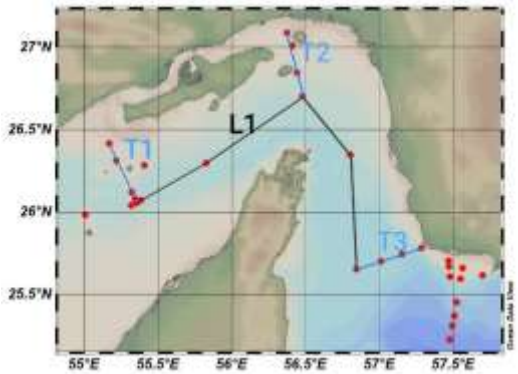

Figure 5. The plotted profiles T1, T2, and T3 illustrate conditions in the western, central, and eastern parts of the Strait of Hormuz, while profile L1 represents a transect from the western to the eastern Strait of Hormuz

Figure 6 shows vertical profiles from the Iranian coast to the central Persian Gulf in both seasons. The winter salinity profile reveals lower surface salinity near the Iranian coast and higher salinity in deeper layers near the central and southern Arabian coasts.

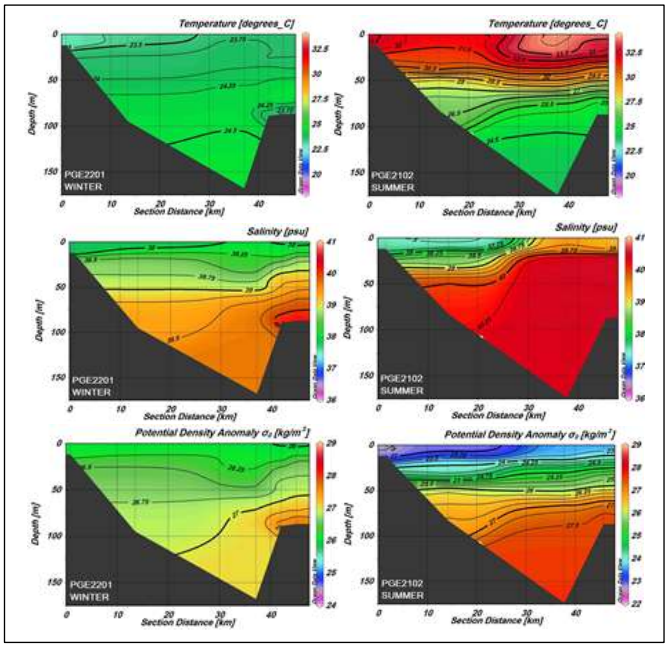

Figure 6. Plotted profiles of salinity, temperature, and potential density anomaly along transect T1 in the western part of the Strait of Hormuz

In summer, low-salinity waters from the northeastern Gulf extend toward the central basin, indicating the inflow of IOSW. Salinity increases from north to south, and also with depth in the eastern Gulf, suggesting the formation of a high-salinity bottom water mass, particularly in the southern Gulf.

The summer temperature profile shows a well-mixed surface layer down to ~20 meters due to turbulence and interaction. The thermocline develops between 30 and 50 meters, marking the transition to cooler, denser waters.

The potential density anomaly profile in summer indicates a progressive increase with depth, with the highest values in the southeastern deep Gulf, confirming the presence of a dense bottom water mass.

The winter profiles in Figure 6, from northeast to southeast, show a gradual salinity increase from surface to bottom in the northeast, rising from 38 psu to over 39 psu near the seabed. Moving from the northwestern Strait of Hormuz to the central Gulf, surface salinity increases slightly to 38.5 psu.

In the central Gulf stations, salinity variation with depth is minimal, remaining just above 40 psu. Near the Iranian coast, a two-layer structure is evident: fresher surface waters overlying saltier bottom waters.

Thermally, lower temperatures are recorded near the Iranian coast, with warmer waters in the central Gulf. Toward the southern coast, temperatures decrease slightly. Temperature inversion is observed in northern stations, where surface waters are cooler than deeper layers, forming a two-layer thermal structure. In the central Gulf, a warm water lens with temperatures near 24°C extends from surface to near-bottom.

Potential density anomaly profiles show a consistent increase from surface to bottom, with a slight rise in density from northern to central stations in the Strait of Hormuz.

Figure 7 illustrates vertical profiles of salinity, temperature, and potential density anomaly from north to central Strait of Hormuz. In summer, the northern strait exhibits homogeneous water properties, with surface salinity decreasing toward the center, likely due to the presence of a fresher water mass extending to ~30 meters depth.

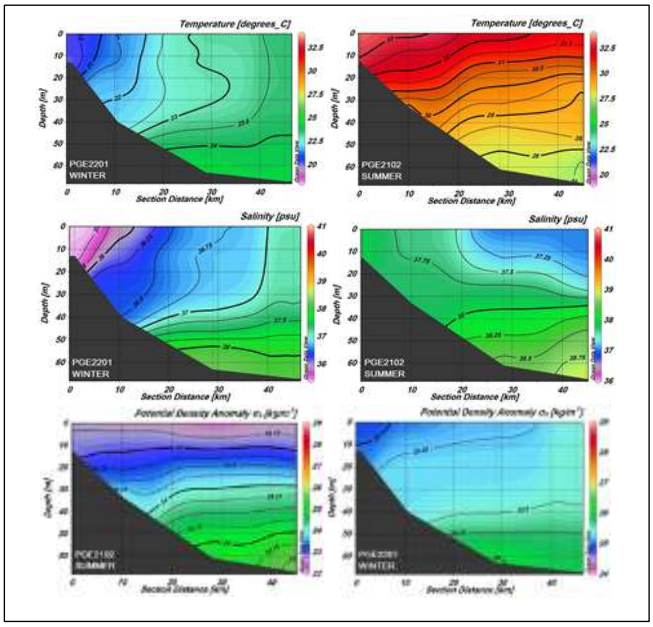

Figure 7. Plotted profiles of salinity, temperature, and potential density anomaly along transect T2 from north to south in the central part of the Strait of Hormuz

In the central strait, salinity increases with depth, forming a strong halocline between 30 and 60 meters. The presence of high-salinity bottom waters indicates the outflow of PGW through the southern and mid-depth layers of the strait.

The temperature section shows higher surface temperatures in the northern strait compared to the center, due to shallower depths and seasonal heating. Surface temperatures decrease toward the center, with the lowest values near the seabed.

Potential density anomaly in the northern strait remains relatively uniform, while in the central strait, density increases with depth.

The bottom panel of Figure 7 shows north–south vertical profiles across central Strait of Hormuz during winter. Northern stations exhibit very low salinity (~35.4 psu), increasing toward the center. This is attributed to rainfall prior to sampling, introducing freshwater into the northern strait.

In central stations, bottom salinity exceeds 38 psu, while surface layers remain below 37 psu, indicating a two-layer structure. In contrast, the northern strait displays a single-layer structure of locally fresh water. The strongest winter halocline is observed between 40 and 60 meters depth.

3.5. Vertical Profiles and Water Mass Structure

Winter temperature measurements in the vertical profile reveal a pronounced thermal inversion in the Strait of Hormuz, where surface waters are colder than deeper layers. A distinct warm water zone is observed below 50 meters near the seabed. A clear horizontal temperature gradient is evident from northern stations toward the central strait. The thermocline in the northern Strait of Hormuz appears inverted, while in the central stations, a uniform temperature layer extends to 50 meters, followed by a slight increase in temperature with depth.

The potential density anomaly (σ_0) profile shows lower density values in the northern stations and higher densities near the bottom in the central Strait of Hormuz. A weak pycnocline is observed between 40 and 60 meters in the central stations. Large portions of this profile are occupied by homogeneous water masses, with density values ranging from 25.2 to 25.4 kg/m³, indicating the presence of uniform water in the mid-strait region.

Figure 8 presents vertical profiles of salinity, temperature, and potential density anomaly from the coastal zone to the central Gulf of Oman. The salinity profile shows higher surface salinity compared to subsurface layers below 25 meters. Between 25 and 80 meters, a low-salinity zone is evident. As the profile extends from the Iranian coast toward the southern and Arabian coasts, salinity increases near the seabed. The compression of isohalines at the terminal station near the bottom indicates the presence of hypersaline PGW, with salinity approaching 40 psu. Above this layer, a low-salinity lens between 40 and 70 meters suggests the intrusion of Indian Ocean Surface Water (IOSW) into the Gulf of Oman.

Temperature variations in this profile are most pronounced between 15 and 40 meters, where a strong vertical gradient and seasonal thermocline are formed. Near the seabed in the central Gulf of Oman, a temperature increase is observed, attributed to the warmer PGW, which contrasts with surrounding waters.

Regarding potential density anomaly, the upper layers exhibit homogeneous density, while between 20 and 40 meters, density increases. The highest density values are found near the bottom in the central Gulf of Oman, where PGW is present.

The lower panel of Figure 8 shows a winter vertical profile across the eastern Strait of Hormuz, from the Iranian coast to the central strait. Salinity remains uniform and below 36.8 psu from the surface to 60 meters. Toward the Iranian coast, salinity remains stable. However, in stations closer to the Arabian coast, salinity increases sharply below 70 meters, reaching over 39.5 psu within the PGW lens.

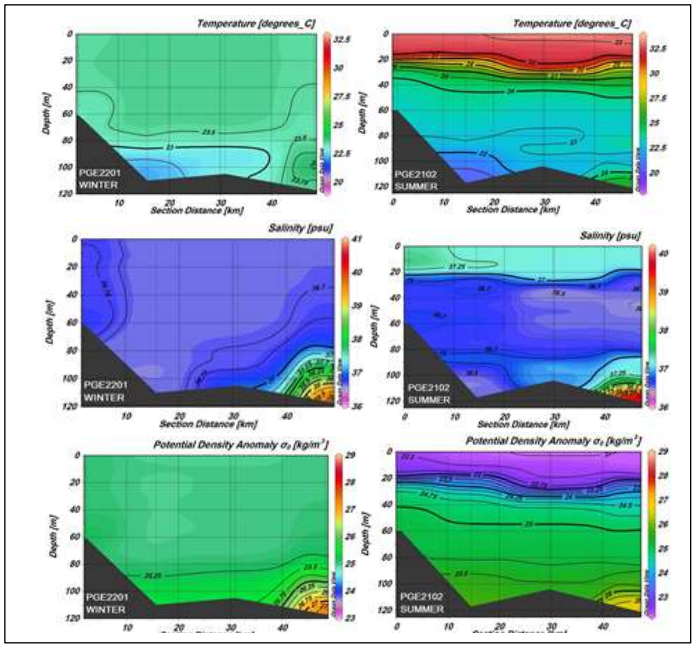

Figure 8. Plotted profiles of salinity, temperature, and potential density anomaly along transect T3 in the eastern part of the Strait of Hormuz

The compression of isohalines and presence of a halocline between 80 and 110 meters are clearly visible in the terminal stations of this transect. Temperature profiles in the eastern Strait of Hormuz show stable values (~23.5°C) in both surface and deep layers up to 70 meters. On the Iranian side, temperatures drop to 22.5°C below 80 meters, while on the Arabian side, temperatures increase with depth, forming a thermal lens (~24°C) at 100 meters—likely associated with PGW intrusion.

The potential density anomaly profile in the eastern Strait of Hormuz reveals a homogeneous layer from surface to 80 meters with density near 25 kg/m³. Below 80 meters, density increases, and in the terminal stations, a sharp rise is observed near the seabed, exceeding 27 kg/m³. This confirms the presence of PGW, characterized by elevated salinity, temperature, and density in the central and southeastern Strait of Hormuz.

Figure 9 displays a vertical profile from west to east across the central Strait of Hormuz. The summer salinity profile shows a progressive increase with depth in the western strait, with values exceeding 40 psu in deeper layers. A clear horizontal salinity gradient from west to east is evident. In the central strait, a two-layer structure emerges: a low-salinity surface layer and a

high-salinity bottom layer, with both horizontal and vertical gradients well defined.

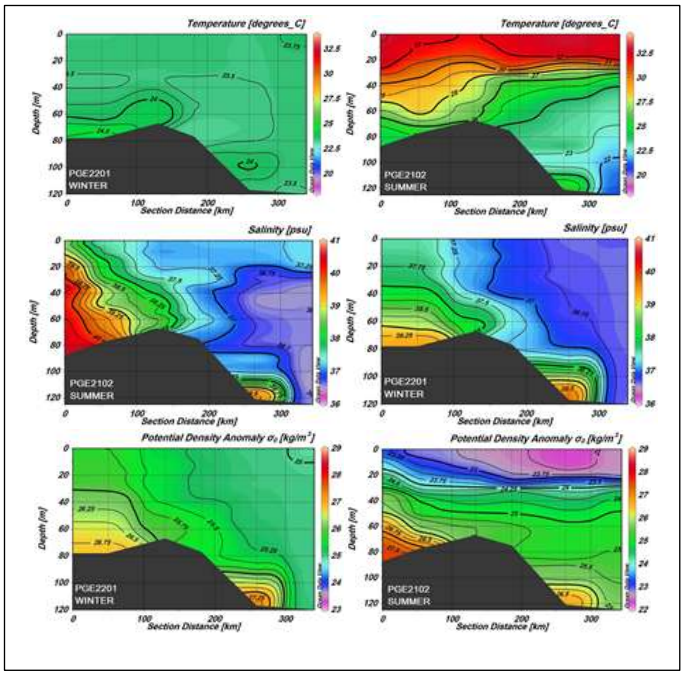

Figure 9. Plotted profiles of salinity, temperature, and potential density anomaly along transect L1 from west to east in the central part of the Strait of Hormuz

In the eastern Strait of Hormuz, a three-layer structure is observed:

- A surface layer with salinity around 37 psu
- An intermediate layer with salinity near 36.5 psu
- A deep layer with salinity exceeding 39 psu

This stratification indicates the presence of a three-layer water mass system extending from the Strait of Hormuz into the Gulf of Oman.

3.6. Potential Density Anomaly Profiles and T–S Diagrams

The vertical profile of potential density anomaly (σ_0) in the western Strait of Hormuz reveals a strong density gradient from surface to near-bottom layers, indicating pronounced water column stratification. In the central strait, a sharp pycnocline is observed at approximately 30 meters, separating low-density surface waters from denser bottom waters. In the eastern Strait of Hormuz, the structure consists of a low-density surface layer, a pycnocline at ~25 meters, and a high-density bottom layer.

The lower panel of Figure 9 presents a winter vertical profile from central eastern Persian Gulf to central western Gulf of Oman. Salinity increases significantly with depth in the eastern Persian Gulf, rising from 37.8 psu to 40 psu at 85 meters. In the Strait of Hormuz, surface salinity is around 37 psu, increasing to 38 psu near 60 meters, then slightly decreasing to 37.5 psu. A saline tongue is observed at 60 meters, extending from the central strait toward the Gulf of Oman, likely indicating intrusion of IOSW. Further into the Gulf of Oman, a saline lens exceeding 39.8 psu is detected, with strong horizontal and vertical salinity gradients, suggesting interaction between IOSW and PGW.

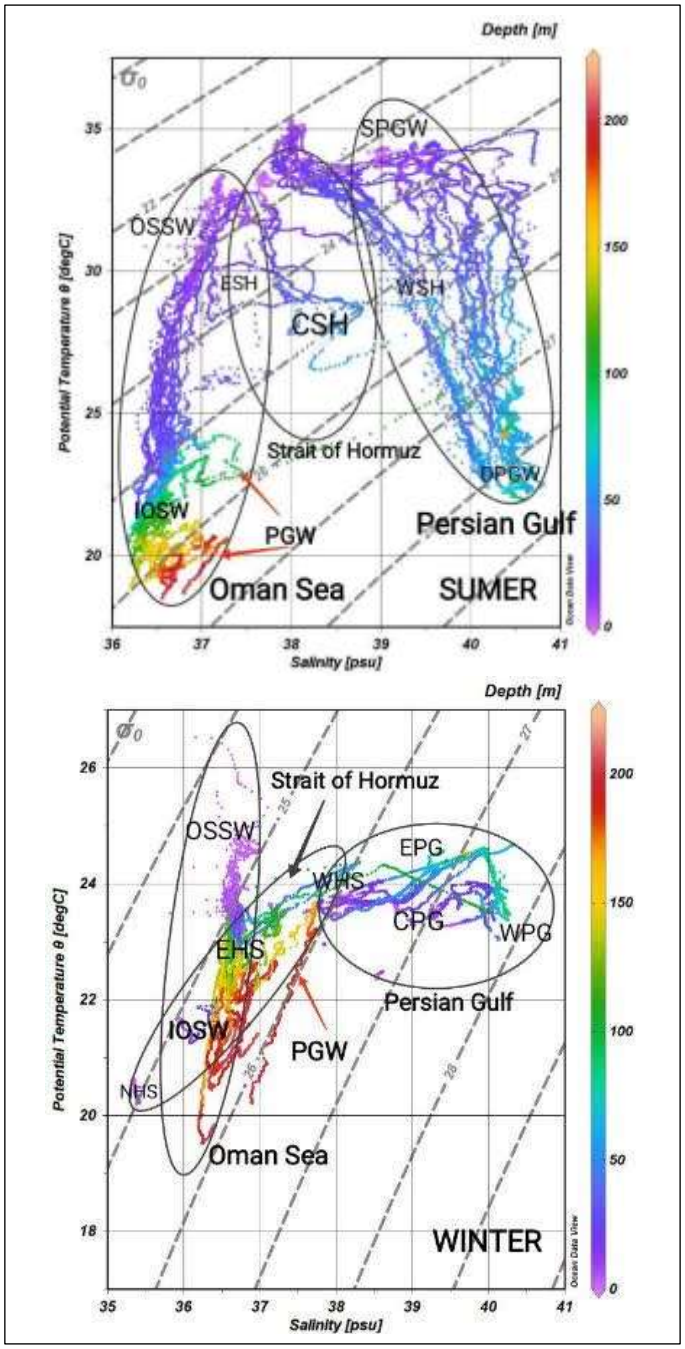

Figure 10. Temperature–salinity (T–S) diagrams for the Persian Gulf, the Strait of Hormuz and the Gulf of Oman during the summer cruise (PGE2102) and the winter cruise (PGE2201)

The temperature profile from eastern Persian Gulf to western Gulf of Oman shows uniform surface temperatures around 33.5°C. In the deeper layers of the western Gulf, temperature increases from 50 meters to the seabed, attributed to the presence of PGW. A similar temperature rise is observed at 80 meters in the eastern Strait of Hormuz, confirming PGW intrusion. This warmer water mass creates thermal inversion

zones, and due to the presence of isothermal layers, no distinct thermocline is observed.

The potential density anomaly profile from eastern Persian Gulf to western Gulf of Oman shows a surface decrease in σ_0 from 26 kg/m³ to 25 kg/m³. In the Persian Gulf, density increases with depth, peaking near the seabed in the Gulf of Oman at 27.5 kg/m³, indicating PGW presence. Toward the central Gulf of Oman, density decreases again, forming a strong horizontal gradient. PGW intrusion generates a pronounced pycnocline between 90 and 115 meters.

3.7. Temperature–Salinity (T–S) Diagrams

T–S diagrams are used to distinguish water mass characteristics. In winter, the Persian Gulf exhibits diverse thermal and salinity conditions across regions. In the northwestern Gulf (WPG), cold and highly saline waters dominate. In the central Gulf (CPG), both salinity and temperature decrease, though some stations show localized increases. In the eastern Gulf (EPG), both temperature and salinity increase with depth. In certain depressions, temperature initially rises with depth before declining, while salinity consistently increases.

In the Strait of Hormuz, northern stations (NHS) show the lowest temperature and salinity due to heavy rainfall prior to sampling. In western stations (WHS), both temperature and salinity increase with depth, though some deep layers show temperature decline. In eastern stations (EHS), salinity is lower than in the west, and temperature remains relatively constant with depth. Temperature increases with depth only in stations influenced by PGW.

In the Gulf of Oman, three distinct water masses are identified:

- Oman Sea Surface Water (OSSW): Low salinity, relatively warm (24–26°C)
- Indian Ocean Surface Water (IOSW): 21–24°C, 36–37 psu, found at 70–140 meters
- Persian Gulf Water (PGW): Very high salinity, temperature up to 24°C, found at 120–180 meters

Overall, T–S diagrams effectively differentiate regional water masses. In winter, PGW is identifiable by higher salinity and lower temperature compared to Oman Sea Water (OSW), which is warmer and less saline. Hormuz Strait Water (HSW) exhibits intermediate salinity and temperature, bridging the Gulf and the open ocean.

4. Summary and Conclusions

Comparative analysis of Persian Gulf water masses in summer and winter reveals that PGW consistently exhibits higher temperatures than surrounding waters in both seasons. In the northwestern Gulf, summer salinity is lower than in winter, while temperatures are warmer in summer and colder in winter. In winter, dense waters form in surface and deep layers of the northwestern Gulf, reaching densities above 30 kg/m³, whereas in summer, densities drop below 26 kg/m³.

Seasonal differences in the Strait of Hormuz are pronounced. In summer, a thermally and salinity-balanced zone forms between the Gulf and the Gulf of Oman. In winter, lower temperatures dominate the northern strait, while moderate temperatures persist in the south. Rainfall in the northern strait disrupts regional water properties during winter sampling.

In terms of stratification, salinity and density layering remain relatively consistent across seasons, but thermal stratification varies significantly. In summer, Persian Gulf waters are warmer than those in the Gulf of Oman, while in winter, the opposite occurs. This is due to the shallowness of the Persian Gulf, which heats and cools more rapidly than the deeper Gulf of Oman. Summer thermoclines are more pronounced in the Gulf of Oman due to its depth, though isotherm compression is stronger in the Persian Gulf. Monsoonal activity in summer enhances mixing in the Gulf of Oman and the Strait of Hormuz, leading to more moderate vertical temperature gradients compared to the Persian Gulf.Results of the work and discussions are presented here.

5. Conclusions

A comparative analysis of Persian Gulf water masses during summer and winter reveals that the Persian Gulf Water (PGW) consistently exhibits higher temperatures than surrounding waters in both the Strait of Hormuz and the Gulf of Oman. In summer, dense and saline waters form near the seabed, while fresher waters occupy the upper layers. In the Gulf of Oman, a three-layer structure emerges, consisting of Oman Sea Surface Water, Indian Ocean Surface Water (IOSW), and outflowing PGW. In contrast, the central water structure of the Strait of Hormuz is notably complex, with pronounced variations in salinity, temperature, and density across vertical layers.

During summer, potential density anomaly (σ_0) increases with depth, forming a dense bottom water mass in the Persian Gulf. In the Gulf of Oman, cooling and salinity elevation contribute to water densification. The PGW core becomes the densest feature in the southwestern Gulf of Oman, while deeper, colder waters below 150 meters further enhance density.

In both seasons, temperature elevation near the seabed in the central Gulf of Oman is attributed to PGW intrusion, which contrasts thermally with ambient waters. In the Persian Gulf, a sharp density increase between 30 and 50 meters creates a compressed pycnocline, which gradually weakens toward the Strait of Hormuz and fully dissipates in the Gulf of Oman.

In winter, PGW reaches salinity levels of 40 psu in the eastern Strait of Hormuz, a value also observed in deep, intermediate, and surface layers of the Persian Gulf. In summer, salinity exceeding 40 psu is confined to deep zones below 30 meters and the northwestern extremity of the Gulf.

Winter density anomaly values in the Gulf of Oman remain relatively stable, but increase toward the Strait of Hormuz. A two-layer structure forms in the central strait, while northern stations, influenced by local low-salinity waters, exhibit a single-layer configuration. The strongest halocline and salinity gradient are observed between 40 and 60 meters.

Thermal inversions are evident in the northern and western Strait of Hormuz during winter, while a warm tongue appears in the eastern sector, driven by PGW with elevated temperature and salinity. From east to west, a broader region of cooler surface waters is observed near the Iranian coast, extending toward the central and southwestern strait, representing the incoming IOSW.

Author contribution

Three authors contributed to this article, whose primary focus was on seasonal stratification patterns in the Persian Gulf resulting from the interaction of water masses during warm and cold seasons in the Persian Gulf and Gulf of Oman.

Acknowledgements

The author gratefully acknowledges the support of the Iranian National Institute for Oceanography and Atmospheric Science, who facilitated the execution of the Persian Gulf Explorer research cruises across the Persian Gulf and Gulf of Oman. Figures were generated using Schlitzer, R. (2021). Ocean Data View (ODV).

8. References

1. Raeisi, A., Bidokhti, A. A., Nazemossadat, S. M. J., and Lari, K. (2020). Impact of mesoscale eddies on climate and environmental changes in the Persian Gulf, *Research in Marine Sciences,* 5 (4), 823-836. https://resmarsci.com/wp-content/uploads/2020/12/Research-in-Marine-Sciences-17-5.pdf

2. Ramak H, soyufjahromi M, Akbari P. Persian Gulf Water mass tracking by surface temperature and salinity properties. joc. 2022; 12 (48):13-28 URL: http://joc.inio.ac.ir/article-1-1616-fa.html

3. Al-Hajri, K. R. (1990). *The circulation of the Arabian (Persian) Gulf: A model study of its dynamics*. The Catholic University of America. https://search.proquest.com/openview/379894904f395b1c07e4a7ad1f9bd0bf/1?pq-origsite=gscholar&cbl=18750&diss=y

4. Reynolds, R. M. (1993). Physical oceanography of the Gulf, Strait of Hormuz, and the Gulf of Oman—Results from the Mt Mitchell expedition. *Marine pollution bulletin*, *27*, 35-59. https://www.sciencedirect.com/science/article/pii/0025326X93900077

5. Pous, S. P., Carton, X., & Lazure, P. (2004). Hydrology and circulation in the Strait of Hormuz and the Gulf of Oman—Results from the GOGP99 Experiment: 1. Strait of Hormuz. *Journal of Geophysical Research: Oceans*, *109*(C12). https://agupubs.onlinelibrary.wiley.com/doi/abs/10.1029/2003JC002145

6. Azizpour, J., Siadatmousavi, S. M., & Chegini, V. (2016). Measurement of tidal and residual currents in the Strait of Hormuz. *Estuarine, Coastal and Shelf Science*, *178*, 101-109. https://www.sciencedirect.com/science/article/abs/pii/S0272771416301780

7. Hunter J. R. (1982). The physical oceanography of the Persian Gulf: a review und theoretical interpretations of previous observations. Paper presented at the First Gulf Conference on Environment and Pollution. Kuwait, 7-9 February 1982.

8. Sonu C. J., (1979). Oceanographic study in the Strait of Hormuz and over the Iranian shelfin the Persian Gulf U.S. Office of Naval Research, Final report, contract no. N00014_76+0720, Tc3675. https://apps.dtic.mil/sti/citations/ADA089144

9. Schott, G. (1918). Ozeanographie und Klimatologie des Persischen Golfes und des Golfes Von Oman. Annalen der Hydrographie und Maritirnen Meteorologic, 4&l-6. https://books.google.com/books?hl=en&lr=&id=uiwzAQAAMAAJ&oi=fnd&pg=PA1&dq=Schott,+G.+(1918).+Ozeanographie+und+Klimatologie+des+Persischen+Golfes+und+des+Golfes+Von+Oman.+Annalen+der+Hydrographie+und+Maritirnen+Meteorologic,+4%26l-6.&ots=LT0gU5JktR&sig=_s2Esb0AjL1IusJD75L2SrJRh14#v=onepage&q&f=false

10. Barlow E. W. (1932) Currents in the Persian Gulf, northern portion of the Arabian Sea, Bay of Bengal etc. I. Summary of previous knowledge. The Marine Observer, 9 (99).

11. Emery K. 0. (1956). Sediments and water of Persian Gulf. Bulletin of the American Association of Petroleum Geologists, 48 (lo), 2354-2383. https://pubs.geoscienceworld.org/aapgbull/article-abstract/40/10/2354/34178

12. Sugden, W. (1963). Some aspects of sedimentation in the Persian Gulf. *Journal of Sedimentary Research*, *33*(2), 355-364. https://pubs.geoscienceworld.org/sepm/jsedres/article-abstract/33/2/355/113017

13. SZEKIELDA, K. H., Salomonson, V., & Allison, L. J. (1972). Rapid variations of sea surface temperature in the Persian Gulf as recorded by Nimbus 2 HRIR. *Limnology and Oceanography*, *17*(2), 307-309. https://aslopubs.onlinelibrary.wiley.com/doi/abs/10.4319/lo.1972.17.2.0307

14. Purser B. H. and E. Seibold, (1973). The principal environmental factors influencing Holocene sedimentation and digenesis in the Persian Gulf. In: The Persian Gulf,

Holocene carbonate sedimentation and digenesis in a shallow epicontinental sea, B. H. Pursur, editor, Springer-Verlag, Berlin, pp. l-9. https://link.springer.com/chapter/10.1007/978-3-642-65545-6_1

15. Grasshoff K. (1976). Review of hydrographical and productivity conditions in the Gulf region in Marine Sciences in the Gulf Area. UNESCO Technical Papers in Marine Science, 26, pp. 39-62. https://ci.nii.ac.jp/naid/10006584248/

16. Sewell, R. B. (1934). The John Murray Expedition to the Arabian Sea. *Nature*, *133*(3351), 86-89. https://ui.adsabs.harvard.edu/abs/1934Natur.133...86S/abstract

17. Emery, W. J., & Meincke, J. (1986). Global water masses-summary and review. *Oceanologica acta*, *9*(4), 383-391. https://archimer.ifremer.fr/doc/00110/22090/19731.pdf

18. Duing W. and P. K. Koske, (1967). Hydrographic observation in the Arabian Sea during the N.E. monsoon period 1964-1965. "Meteor" Forschungsergebnisse A, 8, l-43

19. Duing W. and W. D. Schwill, (1967). Spreading and mixing of the highly saline water of the Red Sea and the Persian Gulf. "Meteor" Forschungsergebnisse A, 8,44-66.

20. Dabestani M, MOHAMMAD MAHDIZADEH M, Azizpour J. Comparison of surface salinity of Persian Gulf water using field data and FVCOM numerical model. joc. 2020; 11 (43):81-87 http://joc.inio.ac.ir/article-1-1602-en.html

21. Emery, W. J., & Meincke, J. (1986). Global water masses-summary and review. *Oceanologica acta*, *9*(4), 383-391. https://archimer.ifremer.fr/doc/00110/22090/19731.pdf

22. Hunter J. R. (1983). Aspects of the dynamics of the residual circulation of the Persian Gulf. In: Coastal oceanography, M.G. Gade, A. Edward and H. Svendsen, editors. Plenum Press, New York, pp. 31-12. https://link.springer.com/chapter/10.1007/978-1-4615-6648-9_3

23. Schlitzer, R. (2021). Ocean data view. http://www.vliz.be/imisdocs/publications/360848.pdf#page=169

24. Swift, S. A., & Bower, A. S. (2003). Formation and circulation of dense water in the Persian/Arabian Gulf. *Journal of Geophysical Research: Oceans*, *108*(C1), 4-1. https://agupubs.onlinelibrary.wiley.com/doi/abs/10.1029/2002JC001360

25. Thoppil, P. G., & Hogan, P. J. (2010). A modeling study of circulation and eddies in the Persian Gulf. Journal of Physical Oceanography, 40(9), 2122-2134. https://journals.ametsoc.org/view/journals/phoc/40/9/2010jpo4227.1.xml

26. Yao, F., & Johns, W. E. (2010). A HYCOM modeling study of the Persian Gulf: 1. Model configurations and surface circulation. Journal of Geophysical Research: Oceans, 115(C11). https://agupubs.onlinelibrary.wiley.com/doi/abs/10.1029/2009JC005781